Overview of RIKEN RI Beam Factory Project

Y. Yano and A. Goto

The Institute of Physical and Chemical Research (RIKEN), Wako, Saitama 351-0198, Japan

T. Katayama

Center for Nuclear Study, School of Science, University of Tokyo, Tanashi, Tokyo 188, Japan

Within the on-going RI Beam Factory project a cascade of a K930-MeV ring cyclotron and a K2500-MeV superconducting ring cyclotron will be constructed as an energy booster of the existing K540-MeV ring cyclotron. With this new cyclotron system the final energy will be increased up to more than 100 MeV/nucleon even for very heavy ions. By the projectile fragmentation these energetic heavy-ion beams are converted into RI (radioisotope) beams covering the whole range of atomic masses and the energies of several hundreds MeV/nucleon. Moreover, this factory will include a next generation of accelerator complex named the multi-use experimental storage rings (MUSES) consisting of an accumulator-cooler ring, a booster synchrotron ring and double storage rings. The MUSES will enable us to conduct various unique colliding experiments. In 1998 fiscal year, the three-year budget has been approved for constructing six sets of superconducting sector magnets for the SRC and the full set of the IRC.

1   Introduction

In recent years the advent of radioisotope (RI) beams has opened up a number of fascinating new fields. To further develop the new fields of science, the RIKEN Accelerator Research Facility (RARF) has undertaken construction of an "RI-Beam Factory," or simply "RIB factory," as a next generation facility that is capable of providing the world's most intense RI beams at energies of several hundreds MeV/nucleon over the whole range of atomic masses.

Figure 1 shows how the RIB factory will look like. This new facility will add new dimensions to the RARF's existing capabilities. At present the RARF has the world-class heavy-ion accelerator complex consisting of a K540-MeV ring cyclotron (RRC) and a couple of different types of the injectors: a variable-frequency Wideröe linac (RILAC) and a K70-MeV AVF cyclotron (AVF). Moreover, its projectile-fragment separator (RIPS) [1] provides the world's most intense light-atomic-mass RI beams. In the factory, a cascade of a K930-MeV intermediate-stage ring cyclotron (IRC) and a K2500-MeV superconducting ring cyclotron (SRC) will be a post-accelerator for the existing RRC. This new cyclotron system will be able to boost the RRC beam's output energy up to 400 MeV/nucleon for light ions and more than 100 MeV/nucleon for very heavy ions. As in the existing RIPS, RI beams will be generated by projectile
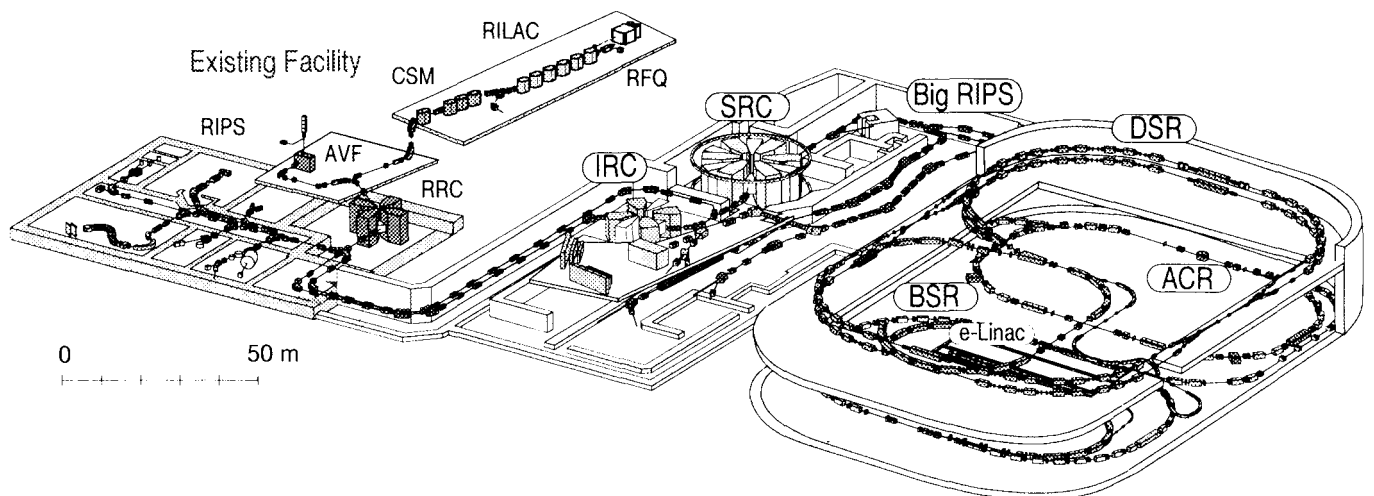

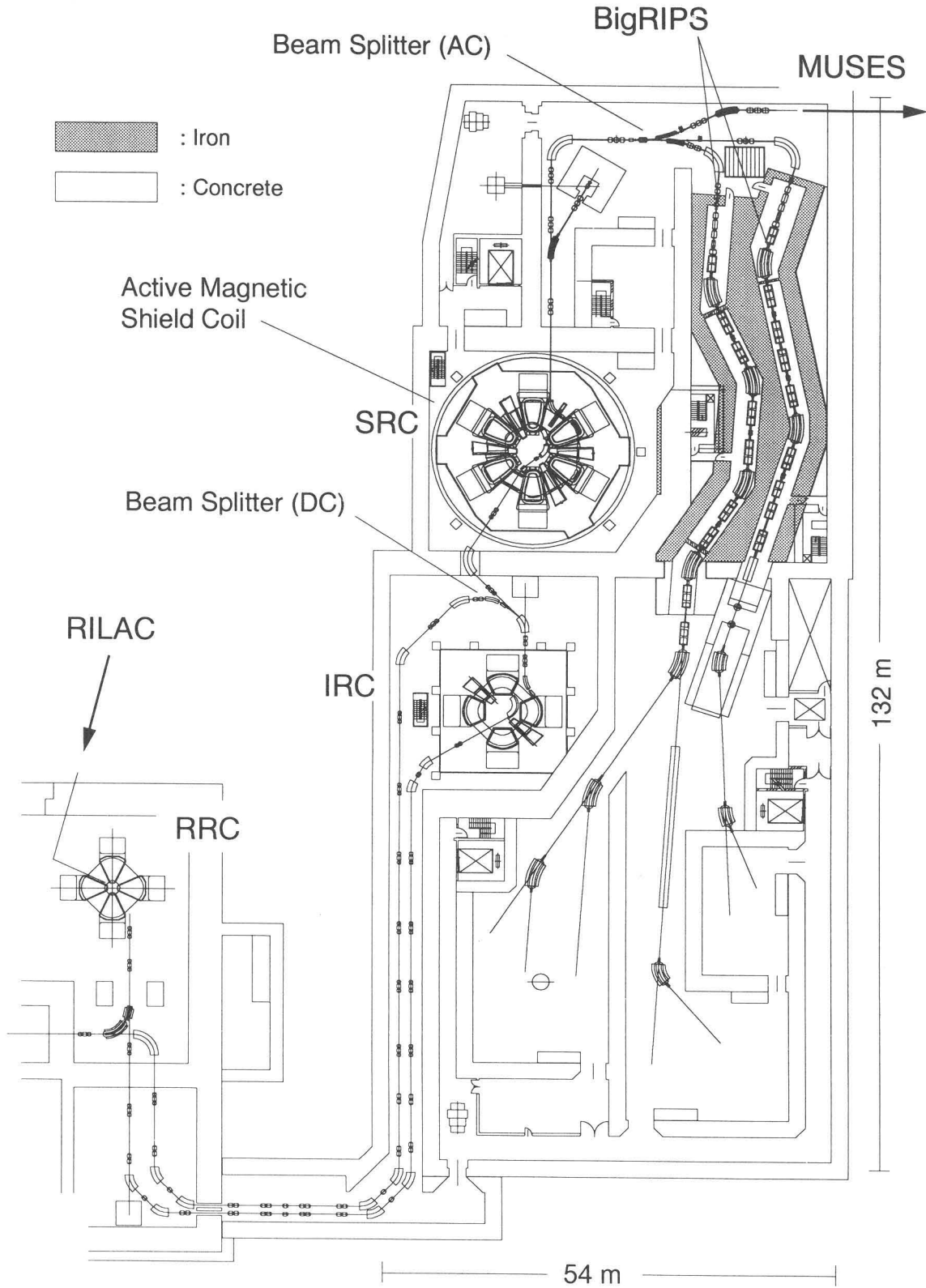Fig. 1 Schematic layout of the RIKEN RI beam factory.

Fig. 2   Drawing of the building that will be constructed in the phase I.

RILAC   (CSM)   RRC   (IRC)   (SRC)

Stripper1   (Stripper2)   (Stripper3)

FCRFQ

18GHz
ECRIS

Accel.
Decel.

BigRIPS

RRC Exp.

18-38 MHz   18-38 MHz   36-76 MHz   18-38 MHz   18-38 MHz   18-38 MHz

$\beta^{out}/\beta^{in} = 4.0$ $\beta^{out}/\beta^{in} = 1.50$ $\beta^{out}/\beta^{in} = 1.506$
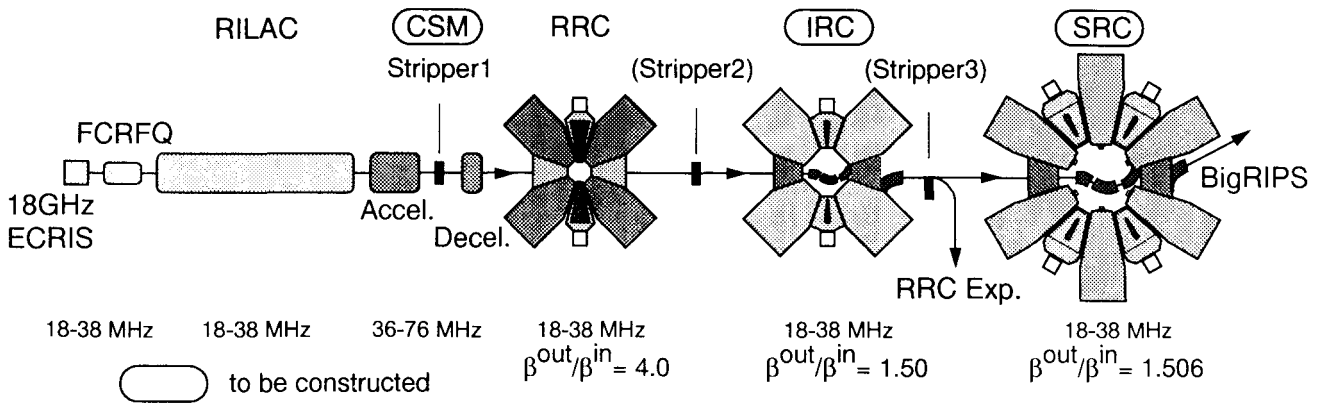
to be constructed

Fig. 3 Conceptual diagram of heavy-ion accelerator complex for RI-beam production.

fragmentation. A BigRIPS will be installed to generate RI beams with much larger magnetic rigidity.

The RIB factory includes a next generation of the multi-use experimental storage rings (MUSES) consisting of an accumulator-cooler ring (ACR), a booster synchrotron ring (BSR) and double storage rings (DSR). MUSES will enable us to conduct various types of unique colliding experiments: ion-ion merging or head-on collisions; collisions of either electrons or X-rays with ion (stable isotope or RI) beams; internal target experiments; and atomic and molecular physics with cooler electron beams.

The construction of the RIB factory is scheduled in two phases: in the first phase, the new cyclotrons, the BigRIPS and the attached experimental installation will be completed; and the MUSES will be constructed in the second. Figure 2 depicts the arrangement of the machines in a building planned for the first phase which will occupy an underground site adjacent to the RARF.

2 Upgrading heavy-ion accelerator complex for high intensity RI beam generation

Figure 3 shows schematic diagram of heavy-ion accelerator complex to produce high intensity RI beams. For efficiently producing RI beams using projectile fragmentation, the primary heavy-ion beam's energy has to be more than 100 MeV/nucleon. In order to exceed this energy even for very heavy ions such as uranium ions, a cascade of powerful cyclotrons will be constructed as an energy booster of the existing RRC. In addition, to realize their intensity enough to produce RI beams with enjoyable intensity to conduct experiments, we are upgrading the RILAC, which serves as the initial-stage accelerator, by developing its new pre-injector system and a charge-state multiplier (CSM). This accelerator complex aims at producing a 100 MeV/nucleon uranium beam with the intensity over 1 pμA.

2.1 Pre-injector for RILAC

The RILAC is stably operational in the acceleration radio-frequency range between 18 MHz and 38 MHz which correspond to 0.6 MeV/nucleon and 2.8 MeV/nucleon, respectively. In order to upgrade the RILAC performance in the beam intensity, its new pre-injector system consisting of a frequency-tunable folded-coaxial RFQ linac (FC-RFQ) equipped with an 18-GHz ECR ion source (ECRIS-18) has been developed. In the recent acceleration tests, the FC-RFQ has successfully covered heavy-ion beams in the energy-mass region required, and the beam transmission efficiency of as high as 92 % was obtained. In addition, high-intensity highly-charged ion beams have been produced by the ECRIS-18 [2].

We have successfully extracted a 25 MeV/nucleon-and 2 pμA-^{40}Ar beam with the beam power of 2kW from the RRC.

2.2 CSM

The CSM consists of an accelerator, a charge stripper and a decelerator. Its functions are to produce higher charge state of ion beams by further increasing the stripping energy and to reduce their magnetic rigidity by decelerating them to the initial energy. With this device the magnetic rigidity of the RILAC beam with a most-probable charge state can be reduced to the acceptable value of the RRC even when the injection velocity into the RRC is increased as shown in Fig. 4. For the accelerator and decelerator sections, variable-frequency drift-tube linacs will be used, whose rf frequency is varied from 36 to 76 MHz. The total accelerating voltage required for the accelerator section is about 26 MV (8 resonators of 16m in total length) and that for the decelerator section is about 11 MV (4 resonators of 8m in total length). The cross section of one unit of the CSM tanks, based on
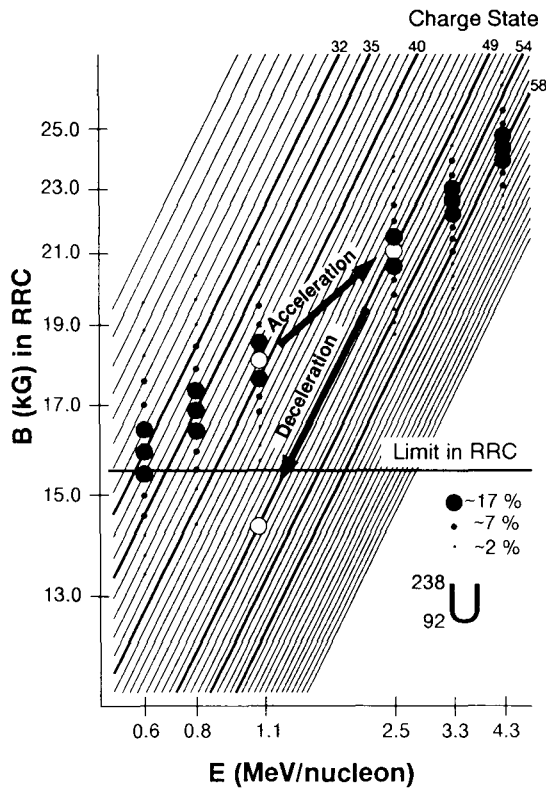
Fig. 4 Principle of the CSM: Size of a dot corresponds to the yields of U ions with respective charge states at the stripping (a carbon foil) energy, E. The ordinate represents the necessary bending power in the RRC.

the IH structure with a movable shorting plate, is shown in Fig. 5. A prototype of this linac will be completed in the spring of 1999.
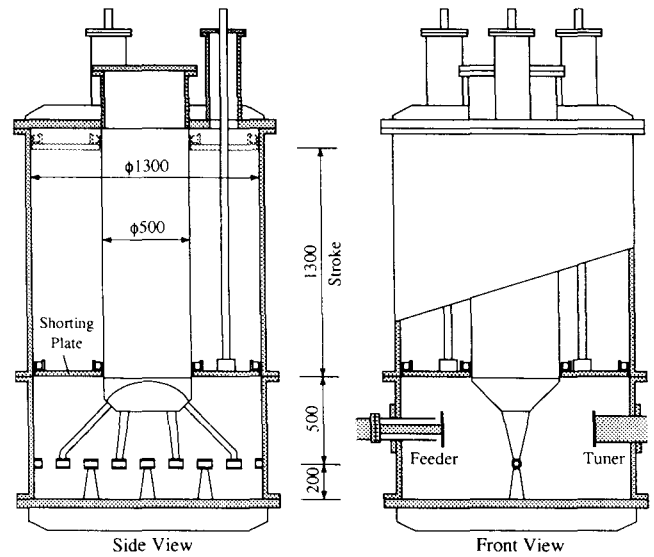
Transmission efficiency through the CSM depends

Fig. 5 Structure of a unit of CSM tanks.

only on charge state distribution behind the charge stripper foil.

2.3 IRC-SRC

The detailed description of the SRC is given in Ref. 3. The maximum beam energy of the SRC is 400 MeV/nucleon for light ions which is achieved at 38 MHz, the maximum radio-frequency in the RILAC. Based on the characteristics of the existing machines, this means that the velocity of the RRC's output beam has to be amplified by a factor of 2.26 by combination of the IRC and the SRC. Harmonic numbers of the IRC and the SRC are chosen to be 7 and 6, respectively, while that of the RRC is 9, considering the maximum magnetic field strength and the
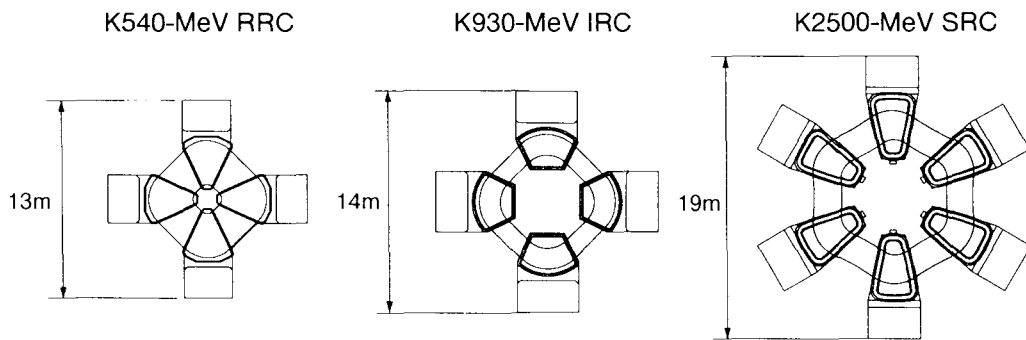
	K540-MeV RRC	K930-MeV IRC	K2500-MeV SRC
Rinj (m)	0.89	2.77	3.56
Rext (m)	3.56	4.15	5.36
Velocity gain	4.0	1.50	1.51
h	9	7	6
B (T)	1.7	1.9	4.4
Weight (ton)	2,100	2,400	4,300

Fig. 6 Comparison of three ring cyclotrons.

Fig. 7 Layout of the SRC with 4 cavities.

Fig. 8 Maximum heavy-ion beam energy obtainable by the IRC and the SRC for ion species with different charge-to-mass ratios, q/A.
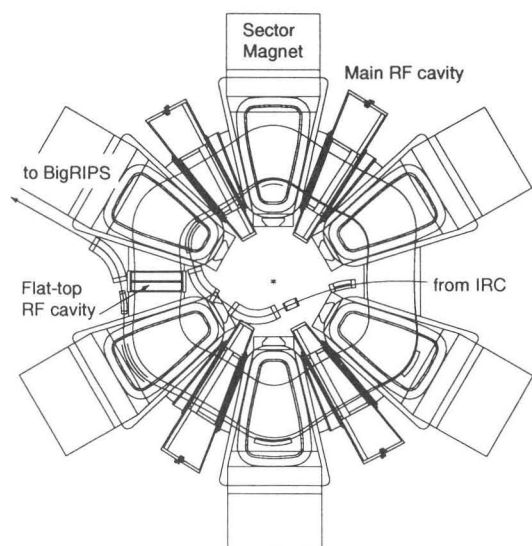
central space to place the injection elements. The mean injection radius of the IRC is taken to be 7/9 times the mean extraction radius of the RRC, and the velocity gain factor of the IRC to be 1.50 (accordingly that of SRC is to be 1.506). On the above conditions, the mean injection and extraction radii of the IRC are 2.77 m and 4.15 m, respectively, and those of the SRC are 3.56 m and 5.36 m, respectively. The sector angles are taken to be 51° for the IRC and 25° for the SRC, based on the beam dynamics study. The radio-frequency of the IRC and the SRC ranges from 18 MHz to 38 MHz which are the same as that of the RILAC and the RRC. The maximum magnetic field strength in the sector magnets is to be 1.9 T for the IRC and 4.3 T for the SRC. This IRC-SRC system boosts the energy of uranium ions from the RRC up to more than 100 MeV/nucleon.

Geometry and characteristics of the IRC and the SRC thus designed are shown in Fig. 6 along with those of the RRC. The structure and size of the IRC are similar to those of the RRC. The rf resonators for the IRC and the SRC are designed by modifying the single-gap resonator of the ring cyclotron at RCNP, Osaka university.

At present we are going to finalize the design of the SRC; and Fig. 7 shows its latest layout with four main cavities and one flat-top cavity.

As shown in Fig. 8 the IRC's maximum energies are 127 MeV/nucleon for light ions up to around Ar, 102 MeV/nucleon for Kr^{30+}, and 58 MeV/nucleon for U^{58+}. The minimum energy is 25 MeV/nucleon. In the SRC the maximum energies are increased to 400 MeV/nucleon for light ions up to around Ar, to 300 MeV/nucleon for Kr^{30+}, to 150 MeV/nucleon for U^{58+} and to 100 MeV/nucleon for U^{49+}. The minimum energy is 60 MeV/nucleon.

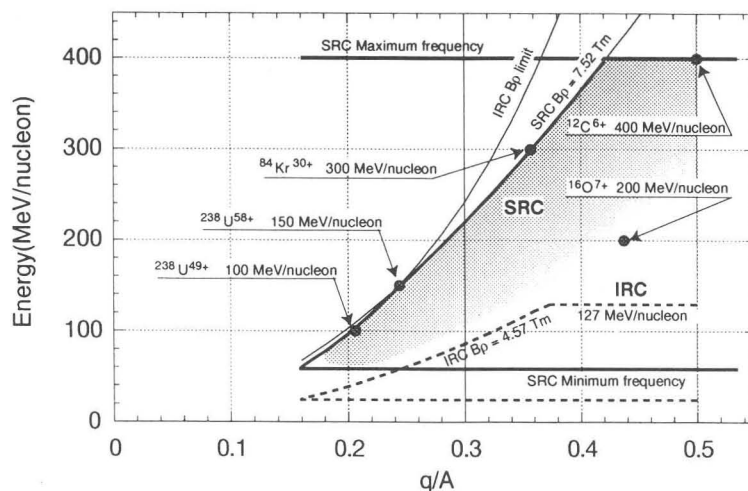We have undertaken the fabrication of a full-scale model sector magnet of the SRC to verify the mechanical and cryogenic design. The completion of this model is scheduled for the end of 1998.

In this two-stage cyclotron scheme the simultaneous utilization of the heavy-ion beams is possible in both of the existing experimental facility and the new facility, when part of the IRC beam is splitted and is transferred back to the existing facility.

3 Multi-Use Experimental Storage Rings (MUSES)

Figure 9 shows schematic diagram of the MUSES. It will be installed downstream the BigRIPS.

The ACR functions for accumulation and cooling of RI beams, and is also used for atomic and molecular physics experiments with a cooler electron beam. The BSR works solely for the acceleration of RI and electron beams. The DSR permits various types of unique colliding experiments: RI - heavy ion merging or head-on collisions; collisions between electron and RI beams; and collisions of RI beams with a high brilliant X-ray emitted from an undulator which is inserted in one ring of the DSR.

3.1 Production of RI Beams

The SRC's heavy-ion beams irradiate a production target and are converted to RI beams through the projectile fragmentation. RI beams generated are the mixture of various RI's; and therefore, they will be purified by means of momentum and charge-state selection at BigRIPS.

Production rates of RI beams were theoretically estimated with the computer code INTENSITY2 [4]. In the code, physical nature of projectile fragmentation process is empirically treated. Kind of primary beam and thickness of the Be production target were optimized so as to obtain the

maximum production rate. Figure 10 shows the result of estimation with the assumption that intensity of the primary heavy-ion beam is 1 pμA, and that the acceptance of the Big-RIPS is ±10 mrad in angle and ±1 % in momentum.

Typical RI-beam quality was also estimated: the momentum spread is ± 0.5 %; the phase width relative to RF frequency is ± 5 degrees; and the transverse emittance is 4.5 π mm·mrad in both horizontal and vertical directions. This beam is transported from the production target point to the injection point of the ACR along the length of 80 m. At the end point of transport line, a debuncher system with a voltage of 4.2 MV and harmonics number of 6 will be installed to reduce the momentum spread to ± 0.15 %.

Fig. 9 Schematic diagram of the MUSES.

3.2 Accumulation and Cooling of RI beams in ACR

Figures 11 and 12 show the time chart for the accumulation process of RI beams in the ACR. RI-beam bunches coming from the BigRIPS are injected into the ACR by means of the multi-turn injection. Then the rf-stacking associated with the beam cooling is performed. Momentum cooling continuously works dur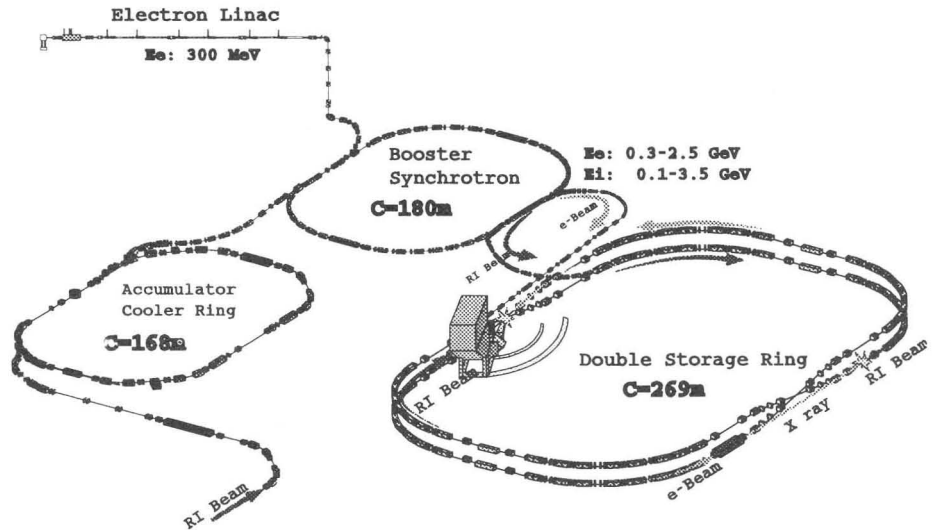ing the rf-stacking. This process is repeated at intervals of the rf-stacking time of 30 ms plus the cooling time τ_{cool} depending on the RI-beam property.

Simulation study for both of the electron cooling and the stochastic cooling of RI beams was done. As a result, it turned out that the stochastic cooling is much faster than the electron cooling. An electron cooler with length of 3.6 m and current density of 0.2 A/cm² gives, for example, the cooling time of 278 s for ^{12}C and 1.98 s for ^{238}U [5], whereas a stochastic cooling system composed of a 1 kW feed-back amplifier with a band width of 2 GHz gives 0.02 s and 5.0 ms with particle number of 10^3 - 10^6 [6], respectively. This is due to the property of the RI beam: the intensity is rather weak; and both of the momentum and emittance spreads are large.

The RI beam accumulated in the ACR decays with its own intrinsic life time τ_{life}. The number N_{total} of the RI ions stored in the ACR after the period of τ_{life} is determined by the balance of the supply rate and the decay rate as shown in Fig. 12. The space charge limit was also considered in the estimation of the maximum number of RI ions stored in the ACR. This limit, however, becomes effective only for RI ions neighboring on the stability line with high production rate.

The accumulated RI beams in the ACR will be fast extracted and one-turn injected into the BSR (see Fig. 12.)

Main parameters of the ACR are listed in Table 1.

3.3 BSR

In the BSR, RI beams will be accelerated to the energy required for the experiment within 0.3 s, and
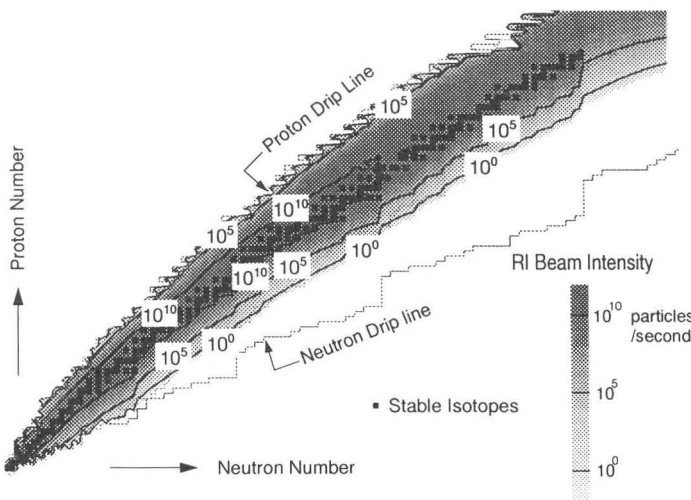

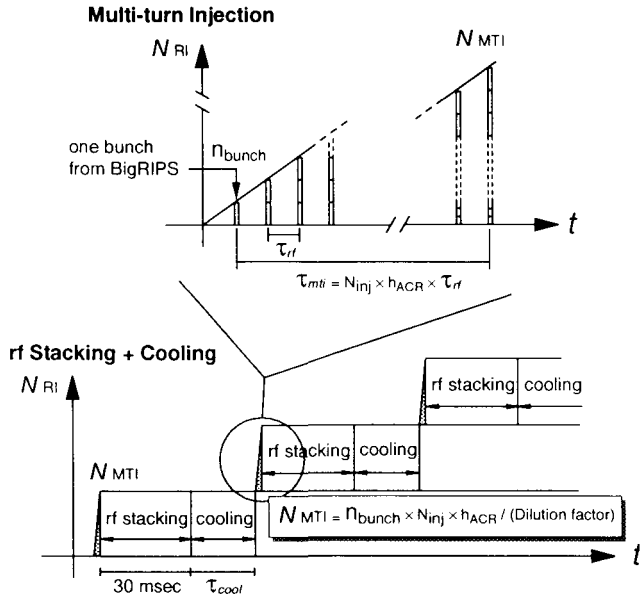Fig. 10 Production rate of RI-beams per 1 pμA primary beam.

Multi-turn Injection

rf Stacking + Cooling

Fig. 11 Time chart of multi-turn injection (top) and rf-stacking plus cooling (bottom) in the ACR. In the figure n_{bunch} denotes the number of RI ions in one bunch coming from the Big-RIPS per τ_{rf} ($=1/38$ MHz–$1/18$ MHz), N_{inj} the number of injected turns ($=\sim40$), and h_{ACR} harmonics of the ACR ($=30$).

then will be one-turn injected into the one ring of the DSR (see Fig. 12.) The maximum energies are: e.g., 1 GeV/nucleon for $^{238}U^{92+}$, 1.5 GeV/nucleon for ions of charge-to-mass ratio (q/A) of 1/2 and 3.5 GeV for protons [7]. The slow-extraction channel will also be prepared.

Electrons are accelerated up to 300 MeV by an electron linac and then injected to the BSR. The BSR boosts the electron energy up to 2.5 GeV at the maximum and supply them to the one ring of the DSR. The expected beam current in the DSR is about 500 mA. In order to make a synchronous collision of electrons and RI ions, the bunch number of electrons are varied from 30 to 75 according to the ion beam energy from 70 MeV/nucleon to 560 MeV/nucleon. The numbers of electrons in a bunch are then 9×10^{10} and 4×10^{10}, respectively.

3.4 DSR

The DSR consists of vertically-stacked two rings of the similar specification. Each lattice structure takes the form of a racetrack to accommodate two long straight sections. These straight sections of one ring vertically intersect those of the other ring at two colliding points: one point is used for the collision between an RI beam and an electron beam at a collision angle of 20 mrad and the other for the merging of RI and stable-ion beams at a merging angle of 170 mrad. RF cavities and beam injection devices are placed at these
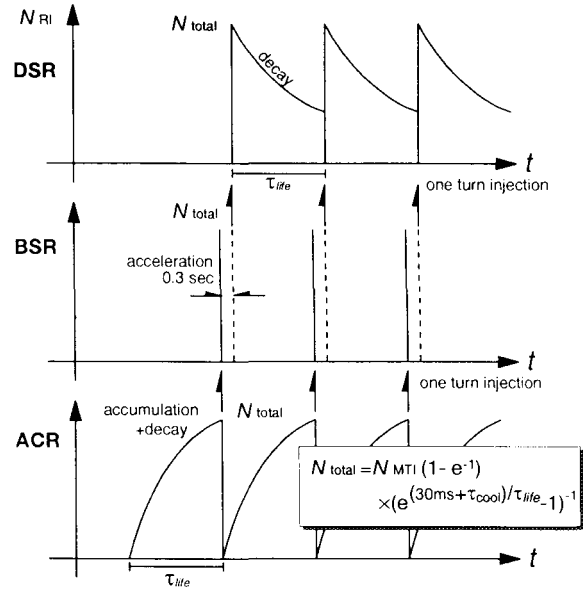

Fig. 12 Time chart of accumulation and acceleration of RI ions in the ACR, BSR and DSR.

Table 1 Main parameters of ACR

Circumference C(m)	168.4836
Max. Magnetic Rigidity $B\rho$(Tm)	7.244
Max. Beam Energy T_{max} (MeV/nucleon)	500(q/A=0.5)
Transition Gamma γ_t	4.987
Betatron Tune Values Qx/Qy	4.555/3.540
Natural Chromaticity $Q'x/Q'y$	-5.058/-6.571
Beam Acceptance (mm·mrad)	125 π
Momentum Acceptance $\Delta P/P$(%)	2.5
Injection Method	
	Multi-turn injection +RF stacking
Beam Cooling Method	
	Stochastic+Electron Cooling

long straight sections. Two short straight sections will be used for electron coolers to suppress the beam instabilities and to make a short-bunch ion beams [8].

The ring circumference is 269.6 m, which is 48/6 times the extraction circumference of the SRC, 33.7 m. It means that the harmonic number of the DSR is 48 while that of the SRC is 6. The maximum $B\rho$–value becomes 14.6 Tm when a dipole field strength is 1.5 T at the maximum. Accordingly the maximum energy is 1.0 GeV/nucleon for U^{92+} ions, 1.5 GeV/nucleon for light ions of q/A=1/2, and 3.5 GeV for protons [9].

One of typical experiments conducted at the DSR is the collision of an RI beam with an electron beam to precisely measure charge-density distribution of unstable

nuclei [10]. In the experiment, one ring of the DSR will be filled with a high-current electron beam of nearly 500 mA with the energy of up to 2.5 GeV. The lattice of this electron ring is designed so that the emittance of electron beam is 10^{-6} π m·rad from the point of view of the luminosity and beam-beam effect. The parameters of the ion ring are different from those of the electron ring because of the difference between lattices of the colliding section in two rings. Another usage of an electron beam is to generate high brilliant X-ray by an undulator inserted in the electron ring [11]. This X-ray will shine Li-like RI ions circulating in the other ring. By detecting fluorescence emission from the ions, new spectroscopy of unstable nuclei will be possible. For this purpose the electron-beam emittance is required to be as small as 10^{-8} π m·rad. This is achieved by forming the Double Bend Achromat (DBA) system in the arc.

Main parameters of the DSR are listed in Table 2.

4   Construction schedule

Within the budget approved in 1998 fiscal year, six sets of superconducting sector magnets for the SRC and a full set of the IRC will be finished three years later. The construction site will be vacant in next spring by removing aged buildings there; and the ground breaking will be started in next fall. According to the present budgetary schedule expected, the first construction phase for the IRC, the SRC, the BigRIPS and the experimental installation will be completed in the spring of 2003. The construction of the MUSES is planned to start in 2003 fiscal year and to be fully finished in 2009.

References

[1]   T. Kubo et al., Nucl. Instrum. Meth., **B70** (1992) 309.
[2]   T. Nakagawa et al.: in this proceedings.
[3]   A. Goto et al.: in this proceedings.
[4]   J.A. Winger et al.: Nucl. Instrum. Meth., **B70** (1992) 380.
[5]   T. Katayama et al.: "MUSES" Conceptual Design Report" to be published.
[6]   N. Inabe et al.: Proc. of EPAC98.
[7]   T. Ohkawa et al.: Proc. of EPAC98.
[8]   M. Takanaka et al.: Proc. of EPAC98.
[9]   N. Inabe et al.: Proc. of EPAC98.
[10] T. Katayama et al., Nucl. Phys., **A626** (1997) 545.
[11] M. Wakasugi et al.: Proc. of EPAC98.

Table 2 Main parameters of DSR

Circumference C(m)	269.568
Max. Magnetic Rigidity $B\rho$(Tm)	14.60
Average Radius R(m)	42.904
Radius of Curvature ρ(m)	9.733
Max. Stored Beam Energy	
Proton (GeV)	3.55
Ion(q/A=0.5)(GeV/nucleon)	1.45
Electron(GeV)	2.5
Operation mode for Electron	
Transition Gamma γ_t	4.857
Betatron Tune Values Qx/Qy	6.754/8.163
Natural Chromaticity $Q'x/Q'y$	-37.7/-90.7
Max. β values $\beta x/\beta y$ (m)	113/750
β values at Intersection point β^*x/β^*y (m)	0.02/0.02
Operation mode for Ion	
Transition Gamma γ_t	5.071
Betatron Tune Values Qx/Qy	6.235/5.018
Natural Chromaticity $Q'x/Q'y$	-62.7/-47.6
Max. β values $\beta x/\beta y$ (m)	1223/970
β values at Intersection point β^*x/β^*y (m)	0.1/0.1